



HAL
open science

Magnetic Confinement Fusion - Plasma Theory: Heating and Current Drive

Rémi Dumont

► **To cite this version:**

Rémi Dumont. Magnetic Confinement Fusion - Plasma Theory: Heating and Current Drive. Encyclopedia of Nuclear Energy, Elsevier, In press, 9780128197257. cea-03134128

HAL Id: cea-03134128

<https://cea.hal.science/cea-03134128>

Submitted on 8 Feb 2021

HAL is a multi-disciplinary open access archive for the deposit and dissemination of scientific research documents, whether they are published or not. The documents may come from teaching and research institutions in France or abroad, or from public or private research centers.

L'archive ouverte pluridisciplinaire **HAL**, est destinée au dépôt et à la diffusion de documents scientifiques de niveau recherche, publiés ou non, émanant des établissements d'enseignement et de recherche français ou étrangers, des laboratoires publics ou privés.

Magnetic Confinement Fusion - Plasma Theory: Heating and Current Drive

R. J. Dumont

CEA, IRFM, F-13108 Saint-Paul-lez-Durance, France

remi.dumont@cea.fr

Abstract

Plasma heating is required to reach and maintain the conditions compatible with power production in magnetic fusion devices. In addition, current drive is essential to the operation and performance of tokamaks. This chapter reviews the main physics processes underlying heating and current drive in the framework of the kinetic theory, in particular radiofrequency wave propagation and absorption, and the collisional relaxation of energetic particles. The self-heating of burning plasmas is described, as well as the main auxiliary heating methods relevant to modern fusion devices, including neutral beam injection and radiofrequency waves in several range of frequencies.

Keywords

Burning plasmas, Coulomb collisions, Current drive, Cyclotron damping, Electron cyclotron (EC) waves, Ion cyclotron (IC) waves, Kinetic theory, Landau damping, Lower hybrid (LH) waves, Neutral beam injection (NBI), Plasma heating, Quasilinear theory, Radiofrequency (RF) waves

I. Introduction

The principle of heating and current drive of magnetic confinement fusion plasmas consists of transferring energy produced by a power source to the plasma species. Whereas heating results in an increase of their temperature, more sophisticated schemes, among which current drive, are used as a means to control the plasma and ensure its state remains optimal with respect to fusion power production. In present day devices, the electrical grid typically supplies this power. On the other hand, the burning plasmas contained in future reactors will essentially be self-sufficient in terms of power: one fifth of the energy produced by the D-T reactions comes in the form of kinetic energy of ^4He (alpha) particles, which is much larger than the average energy of any other species present in the plasma. Upon collisional slowing-down on the background species, the alpha particles will yield their energy to the plasma. A fraction of the fusion power produced in-situ will also be recirculated to feed external generators used mainly for plasma control. These considerations apply to the two main classes of reactors envisaged today, i.e. tokamaks ([Zohm, 2020](#)) and stellarators ([Yamada, 2020](#)). In modern fusion installations, there exist two main classes of external power sources: 1) radiofrequency systems, 2) neutral beam injection systems.

Every radiofrequency (RF)-based heating and current drive method relies on an external power source on the one hand and an adapted antenna located near the plasma edge on the other hand. How this power travels between the source and the antenna depends on the frequency range. In an optical-like description of the process, in all cases, an electromagnetic wave eventually leaves the antenna and propagates to the plasma core where it is absorbed by the plasma species by two main non-collisional mechanisms: Landau damping and cyclotron damping. These mechanisms result in the direct damping of the wave power by one or several thermal species that will be heated as a result, and/or the creation of energetic particle populations (i.e. particles with typical energies much larger than the thermal energy characterizing the background plasma species) which eventually heat the plasma by collisional relaxation.

Neutral beam injection (NBI) consists of producing high-energy ions in an external accelerator, and neutralizing them at the end of the acceleration process. These neutral particles, being immune to the effects of the magnetic trap in which the thermal species are confined, can penetrate deep in the plasma. In this process, the vast majority of the energetic particles are re-ionized. Since the re-ionization occurs when the injected particle energy is much larger than that of the thermal species, the result is a population of energetic ions that eventually slow down through collisions with the background particles, to which they transfer their energy.

Finally, fusion products are usually born at very high energies, the most prominent being the alpha particles from D-T reactions born around 3.5MeV. The relaxation process is essentially similar to the one taking place for NBI ions, i.e. results in a transfer of the fusion product energy to the background electrons and/or fuel ions and the subsequent heating of the plasma. A plasma can be qualified as “burning” when this self-heating process provides a source sufficient for the fusion reactions to be maintained with little or no input required from auxiliary power sources.

Current drive is essential in tokamaks, which require the presence of a poloidal magnetic field produced by the toroidal plasma current ([Wesson, 2011](#)). This current can be induced in the plasma by the central solenoid, part of the poloidal circuit (ohmic current) - an inherently non-stationary process - or self-generated by the plasma pressure gradient (*bootstrap current*). The ohmic and bootstrap

currents generally need to be supplemented by additional sources to achieve stationary plasma discharges. Furthermore, current profile control is known to be beneficial in terms of plasma stability and performance (Jenko, 2020), but requires a level of flexibility only achievable with external current drive sources. Some NBI systems are flexible enough for part of the energy to be injected parallel to the magnetic field, which has the effect of driving toroidal current, albeit with a limited flexibility in terms of current profile control. RF wave systems have also been applied for non-inductive current drive for several decades, and are planned to be used for this application in next-step devices. In stellarators, the magnetic field, including its poloidal components, is entirely generated by the coil system, resulting in more modest requirements in terms of external current drive. Nevertheless, the capability to drive non-inductive current is still desirable to compensate for the self-generated bootstrap current.

A global summary of the process of heating and current drive is shown in Figure 1.

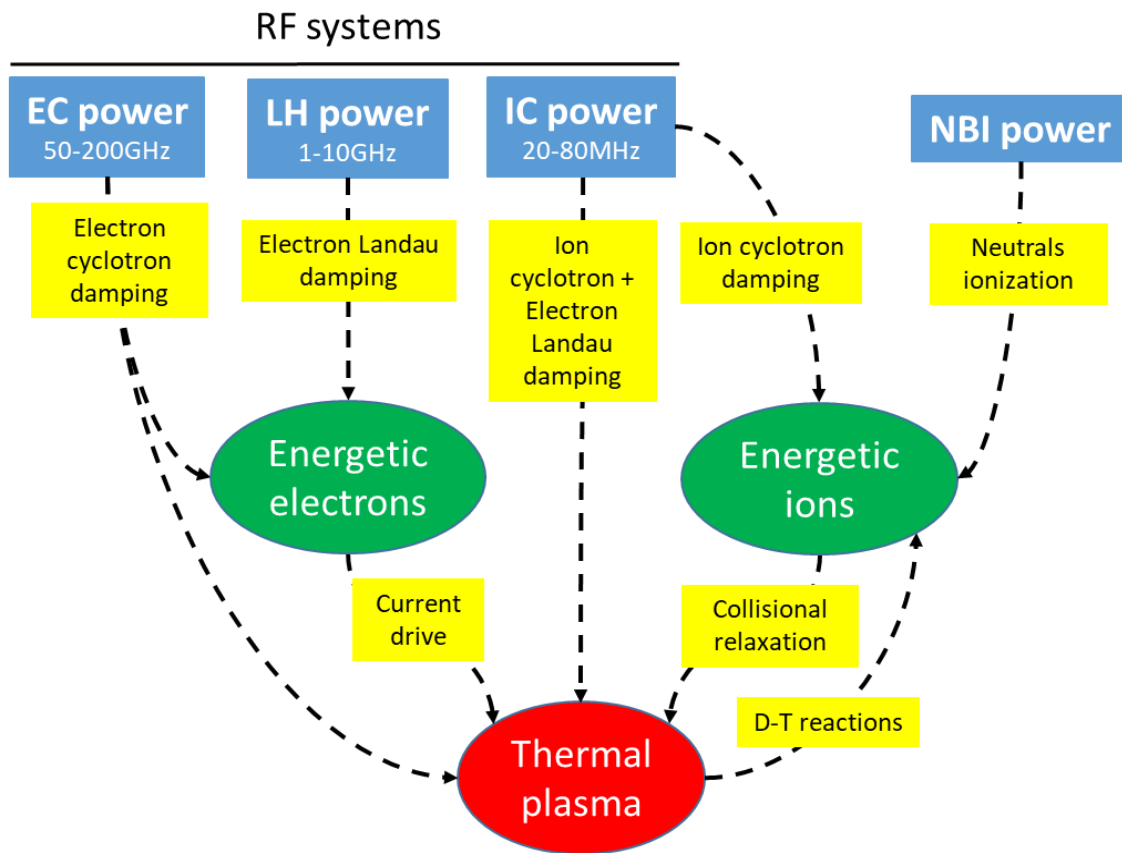


Figure 1: Summary of the main heating and current drive sources in modern magnetically confined fusion plasmas.

II. Kinetic theory elements

Heating and current drive results in modifications of the velocity distribution function, f_s , of a given plasma species, denoted s . From this quantity, it is possible to construct the so-called fluid moments (Sarazin, 2020), which include the density, $n_s = \int d^3\mathbf{v} f_s$, the current, $\mathbf{j}_s = q_s \int d^3\mathbf{v} \mathbf{v} f_s$, and the temperature, $T_s = \int d^3\mathbf{v} m v^2 f_s / 2$. To lowest order, plasma heating and current drive from external sources results in modifications of these three fluid quantities. Clearly, the knowledge of f_s is therefore the first and most important element of the description of the physics processes involved. Furthermore, the RF wave heating and current drive processes involve wave-particle resonances which are dependent on the

particle velocities on an individual basis (as opposed to the fluid velocity, which is a macroscopically averaged quantity). As a result, the kinetic theory is the appropriate framework in which these phenomena must be described.

1. Fokker-Planck equation

The *Fokker-Planck equation* is the classical tool employed to describe heating and current drive processes ([Brambilla, 1998](#)). It is derived from the more generic kinetic *Boltzmann equation* assuming that Coulomb collisions result in multiple small angle deviations for a given particle, a valid assumption in the context of magnetically confined fusion plasmas. Formally, this equation takes the form of an evolution equation for the distribution function, f_s , in velocity space under the effects of collisions, particle source and particle losses:

$$df_s/dt=C(f_s)+S_s-L_s. \quad (1)$$

S_s is the particle source (relevant in the case of NBI and/or fusion-born alphas, in which new particles are permanently injected in the system) and L_s is a loss term describing the particles leaving the system by various mechanisms (orbit losses, charge exchange...), while $C(f_s)$ represents the effect of collisions, and can be written in the form:

$$C(f_s)=-\nabla_v \cdot (\langle \Delta \mathbf{v} \rangle / \tau_c f_s) + 1/2 \nabla_v \nabla_v \cdot (\langle \Delta \mathbf{v} \Delta \mathbf{v} \rangle / \tau_c f_s). \quad (2)$$

τ_c is a collision time. ∇_v is a differential operator with respect to components of the velocity, \mathbf{v} . In Eq. 2, the first term represents a convection process, whereas the second term represents a random walk. The Fokker-Planck equation therefore describes a convection-diffusion process taking place in velocity space. The quantity $F \equiv \langle \Delta \mathbf{v} \rangle / \tau_c$ is called the coefficient of dynamic friction, whereas $\mathbf{D} \equiv \langle \Delta \mathbf{v} \Delta \mathbf{v} \rangle / \tau_c$ is the diffusion tensor.

In its generic form - consistent with the assumptions made to obtain the Fokker-Planck equation -, F and \mathbf{D} involve all species present in the plasma, making C a non-linear operator which can be quite complex to evaluate. It becomes much more tractable when assuming that the background species, i.e. all species but the heated one(s) have Maxwellian velocity distributions, an assumption often legitimate in the context of heating and current drive in magnetic fusion plasmas.

2. Collisional processes

As described previously, the Fokker-Planck equation (1) describes the collisional processes governing the relaxation of any energetic particle population, and hence the energy transfers taking place between this population and the background plasma species ([Goldston and Rutherford, 1995](#)). This equation can be solved efficiently on any modern computer using various numerical methods, typically in a Monte Carlo form, or using finite differences/elements. However, much insight into the relaxation process itself can be gained by examining the relaxation of a single test ion on the background plasma species, which are assumed fixed. From the coefficients $\langle \Delta \mathbf{v} \rangle$ and $\langle \Delta \mathbf{v} \Delta \mathbf{v} \rangle$ derived to construct the collisional term (Eq. 2), trajectories in velocity space of an ion with charge number, Z_f , and mass number, A_f , injected (or born) at a given velocity, V_f , and undergoing the influence of Coulomb collisions can be computed.

In the range of energies relevant to energetic ions (NBI or fusion-born), V_f always satisfies $v_{th,i} \ll V_f \ll v_{th,e}$, with $v_{th,i}^2 \equiv 2k_B T_i / m_i$ and $v_{th,e}^2 \equiv 2k_B T_e / m_e$ the (squared) thermal velocities of background ions (of mass m_i) and electrons (of mass m_e). T_e and T_i are the corresponding temperatures and k_B is

the Boltzmann constant. Using this assumption, the dominant collisional processes are found to be 1) a decrease of the test ion velocity resulting from the collisional friction against the background species; 2) a scattering of the test ion pitch-angle (relative to the magnetic field), i.e. a modification of the direction of its velocity with respect to its initial velocity.

A closer examination of the magnitude of these processes allows three important quantities to be identified: 1) the Spitzer slowing-down time (in seconds), $\tau_{se} \equiv 6.32 \times 10^{14} (A_f/Z_f^2) (T_e^{3/2}/n_e) \ln(\Lambda)$, with $\ln(\Lambda)$ the *Coulomb logarithm* and T_e (resp. n_e) the background electron temperature in eV (resp. density in m^{-3}); 2) the critical energy, $E_c \equiv 14.8 (Z_i^2/A_i) A_f T_e$, with A_i and Z_i the background ion mass and charge number; 3) the thermalization time, $\tau_{th} \equiv \tau_{se} \ln(1 + (E_f/E_c)^{3/2})/3$. The Spitzer time describes the rate of change of the test particle velocity caused by the friction on background electrons, i.e. $dv_f/dt = v_f/\tau_{se}$ (i.e. assuming only electrons are involved in the slowing-down process). The critical velocity corresponds to the limit below which pitch-angle scattering and drag by background ions exceeds the scattering and drag caused by electrons. When the test ion reaches E_c , both the background electrons and ions contribute equally to its slowing down. However, the fact that the masses of the test and background ions are not very different also induces significant pitch-angle scattering by the latter. The corresponding decrease in the test particle energy does not result in background plasma heating, but rather in an increased spread in the energetic population velocities. Finally, the thermalization time corresponds to the delay for the test ion to reach the thermal velocities. It should be noted that τ_{th} and τ_{se} can be quite different, as illustrated by the data shown in *Table 1*.

3. Quasilinear description of RF heating

The first step towards describing plasma heating by RF waves is to solve the wave equation for the wave electric field, \mathbf{E} . The wave magnetic field, \mathbf{B} , can always be deduced from \mathbf{E} using Maxwell's equations. Assuming a time-harmonic field varying at an angular frequency, ω (imposed by the generator), i.e. $\mathbf{E} \propto \exp(-i\omega t)$, with t the time, the wave equation is a straightforward consequence of Maxwell's equations, and is written here in the symbolic form:

$$\nabla \times \nabla \times \mathbf{E} - \omega^2/c^2 (\mathbf{E} + i\mathbf{J}_p/\omega \epsilon_0) = i\omega \mu_0 \mathbf{J}_{ant}. \quad (3)$$

In this expression, ∇ is a differential operator (in real space), μ_0 is the vacuum permeability, ϵ_0 the vacuum permittivity, and c is the speed of light. \mathbf{J}_{ant} represents the boundary condition imposed by the antenna. Despite its apparent simplicity, this equation is quite complicated because the response plasma current, $\mathbf{J}_p = \mathbf{J}_p(\mathbf{E})$, has a complex, temporally and spatially non-local, dependence on the wave electromagnetic field. A first simplification occurs assuming that this dependence is linear, a hypothesis generally valid in the context of plasma heating and current drive, where the electromagnetic field is a perturbation for the magnetically confined plasma.

Another source of difficulty related to Eq. 3 is the fact that \mathbf{J}_p depends itself on the distribution function of the various plasma species, including the species which directly absorb the injected power. In other words, it is often necessary to solve the wave equation and an equation to describe the modification of the distribution function in a self-consistent fashion. This two-step approach relies on the fact that the timescales related to the wave propagation and damping are small compared to the timescales related to the secular modifications of the distribution function and Coulomb collisions, which correspond to the macroscopic modifications of the plasma caused by the wave power.

Including RF wave effects on the distribution function requires additional assumptions with respect to those made to derive the Fokker-Planck equation (Eq. 1). The *quasilinear equation* is obtained from the *Vlasov equation* assuming that the non-linear effect of the wave on the distribution function is the product of interactions taking place between the wave field, as deduced from the linearized wave equation (Eq. 3) on the one hand, and of the linear plasma response on the other hand, hence the name quasilinear. This procedure requires an averaging over space (resp. time) scales larger than the wavelength, λ (resp. wave period τ), to eliminate all terms varying on the small space scale, λ , and fast time scale, τ . This quasilinear equation - customarily also referred to as Fokker-Planck equation - therefore applies to F_s , the time and space-averaged version of f_s . Following this procedure, it can be written in the form:

$$dF_s/dt=C(F_s)+Q(F_s)+S_s-L_s. \quad (4)$$

Q is the quasilinear operator, and represents the effect of the waves interacting with the particles of species s on the corresponding distribution function, F_s . In the framework of the quasilinear theory, this term also takes the form of diffusion/friction term involving a quasilinear diffusion tensor, \mathbf{D}_{ql} :

$$Q(F_s)=\nabla_v \cdot (\mathbf{D}_{ql} \cdot \nabla_v F_s). \quad (5)$$

Depending on the level of sophistication of the description used, Q can have a rather complicated form. Important features of the quasilinear operator can nevertheless be isolated by writing any of its components in the symbolic form:

$$D_{ql}=A \sum_p |\mathbf{d}^{(p)}(\mathbf{E})|^2 \delta(\omega - p\Omega_{cs} - k_{//}v_{//}). \quad (6)$$

In this expression, A is a constant. $\mathbf{d}^{(p)}(\mathbf{E})$ is a differential operator acting on the electromagnetic field and $k_{//}$ is the projection of the wave vector in the direction parallel to the magnetic field lines. These two elements are essentially representative of the wave field. $\Omega_{cs}=q_s B_0/m_s$ is the (algebraic) cyclotron frequency, i.e. the frequency of the cyclotron motion of the considered particles (with charge, q_s , and mass, m_s) around the magnetic field line. Ω_{cs} and $v_{//}$, the particle velocity along the field line, are characteristics of the interacting particles trajectories. p , the harmonic number, is an integer which can have either sign, or be 0. $\delta(\omega - p\Omega_{cs} - k_{//}v_{//})$ is non-zero only when the particles are resonant with the wave, i.e. when the wave-particle resonance condition, $\omega = p\Omega_{cs} + k_{//}v_{//}$, is satisfied.

III. RF wave propagation and damping

In RF heating processes, generators located at some distance from the plasma confinement device generate oscillating currents. Depending on the frequency range, the corresponding power is transported to an antenna located inside the vacuum vessel, usually close to the plasma edge (i.e. within several cm). The wave coupling is the process by which the power emanating from the radiating structure in the form of a vacuum electromagnetic wave is transferred to the plasma species. This electromagnetic wave can excite plasma waves of various types: 1) Electromagnetic waves are waves for which the propagation does not rely on the plasma species. 2) Electrostatic waves are characterized by an oscillating electric field in the direction of propagation. This electric field induces an oscillating plasma current and associated space charge, which itself is responsible for a response electric field further away in the plasma. 3) Magnetohydrodynamic (MHD) waves are characterized by an oscillating magnetic field which induces a plasma current, itself inducing a magnetic field further away in the plasma. It should be emphasized that such a separation is an idealized view: actual plasma waves

generally involve several of these processes at the same time ([Stix, 1992](#)). As a result, the separation between the reactive part of the wave power, reversibly exchanged between the electromagnetic field and the plasma species and therefore linked to wave propagation, and the resistive part of the wave power, irreversibly transferred to the plasma species and therefore responsible for plasma heating, is in practice a delicate task ([Swanson, 2003](#)).

1. Wave propagation

There exist several methods to solve the wave equation, Eq. 3. When the wavelength λ remains much smaller than the typical space scales characterizing the plasma equilibrium quantities, L_B , the *WKB approximation* is applicable, allowing Eq. 3 to be solved by ray-tracing or beam-tracing (quasi-optical methods). On the other hand, regimes in which λ becomes comparable to, or larger than, L_B , or in which the wave undergoes reflection or resonance phenomena during its propagation make it necessary to solve Eq. 3 directly, by resorting to a full-wave approach. Although more intensive numerically, modern computers allow this type of calculation to be performed in a routine fashion, including for higher frequency waves.

However, in all cases, considerable insight can be gained by analyzing the dispersion relation corresponding to the wave equation. This relation is obtained by assuming that the plasma is stationary and homogeneous. Whereas the former assumption is relatively safe in the context of plasma heating by RF waves, the homogeneity hypothesis is often questionable. Despite this limitation, the dispersion relation is always very useful to analyse wave propagation in plasmas. Writing the local electric field as a monochromatic plane wave characterized by wavevector, \mathbf{k} , i.e. $\mathbf{E}(\mathbf{r},t) \propto \exp(i(\mathbf{k}\cdot\mathbf{r}-\omega t))$, the dispersion relation takes the generic form, $D(\omega,\mathbf{k})=0$, and therefore expresses an implicit relation between the wave frequency, ω , and wavevector, \mathbf{k} , or equivalently the refractive index, $\mathbf{N} \equiv \mathbf{k}c/\omega$. Usually, multiple solutions to $D(\omega,\mathbf{N})=0$ at a given point in the medium are possible, indicating the potential presence of several modes, each one characterized by a different dependence of \mathbf{N} on the plasma parameters (density, magnetic field...). Once a given solution (or mode) is chosen, the dispersion relation can be used in the wave equation to deduce the wave polarization, i.e. the ratio between the various components of the wave electromagnetic field. Among these components, the parallel, $E_{//}$, left-handed, E_+ , and right-handed, E_- , turn out to be of particular importance because they physically correspond to a wavefield oscillating in a direction parallel to the magnetic field ($E_{//}$), and rotating in the same direction as ions (E_+) or electrons (E_-).

In magnetically confined plasmas, the projection of \mathbf{N} along the magnetic field, $N_{//}$, is essentially determined by the antenna geometry, and usually does not vary much as the wave propagates. The perpendicular component, N_{\perp} , on the other hand, largely depends on the plasma parameters. It is instructive to investigate wave propagation in terms of N_{\perp} in the context of the cold plasma theory, in which all species are assumed to have zero temperature. In such plasmas, the dispersion relation can be written as $D(\omega,N_{\perp})=A(x)N_{\perp}^4+B(x)N_{\perp}^2+C(x)$, where the coefficients A , B and C are function of the local plasma parameters ([Stix, 1992](#)), parametrized here by the variable x . The consequence is that only two modes can exist at a given point, x , in a cold plasma. Furthermore, there may exist points verifying $N_{\perp}^2(x)=0$, called cut-offs. In this situation, the wave can only propagate up to the cut-off where it is reflected. Points such that $N_{\perp}^2(x) \rightarrow \infty$ are called resonances.

The inclusion of finite temperature effects in the model regularizes the singular behavior observed at cold resonances. Wave absorption, a phenomenon absent in the cold plasma theory, takes place and

results in an irreversible power transfer through the resonance mechanism involving the wave field and the particle motion. Retaining thermal effects also has the consequence of allowing more than two modes to propagate in the plasma. In particular, it is possible to encounter situations for which two modes characterized by $N_{\perp 1}$ and $N_{\perp 2}$ propagating independently reach a point such as $N_{\perp 1} = N_{\perp 2}$. In this case, part of the wave power in a given mode can be partially transferred to another mode, in a process called mode-conversion.

In magnetic fusion plasmas, these three processes i) wave cut-off, ii) resonant wave absorption and iii) mode conversion, are quite prevalent and therefore need to be included in any description of wave propagation and absorption ([Stix, 1992](#)).

2. Wave absorption

As discussed previously (see section “Quasilinear description of RF heating”), wave-particle resonance occurs when parameters characterizing a wave (ω , k_{\parallel}) and parameters characterizing a given plasma species are such that a resonance condition is fulfilled. k_{\perp} , on the other hand, is determined by the dispersion relation. Typically, such a resonance occurs when the wave frequency matches the local gyration motion of electrons or ions, $\omega = \Omega_{cs} + k_{\parallel} v_{\parallel}$ (cyclotron resonance), one of its harmonics, $\omega = p\Omega_{cs} + k_{\parallel} v_{\parallel}$ (harmonic cyclotron resonance, with $p > 1$) or the parallel particle motion, $\omega = k_{\parallel} v_{\parallel}$ (Cerenkov resonance). A synchronization process takes place between the wave-field and the particle motion. However, this process is reversible by nature. The transformation of reactive power to resistive power through the wave-particle resonance requires one or several mechanisms responsible for decorrelating the field oscillation from the plasma particle response. These processes are often referred to under the generic term of phase-mixing mechanisms. One such decorrelation process is the Coulomb collisions themselves. By their stochastic nature, collisions are clearly able to destroy any wave/particle correlations. However, experimental evidence pointed to the possibility of wave damping even in collisionless plasmas, triggering an intense effort to interpret these results and identify non-collisional damping mechanisms.

a) Landau damping

Non-collisional damping has been the center of vigorous debates. Several mathematical derivations have been put forward to describe this phenomenon. However, L. Landau is to be credited for the unambiguous explanation of this effect in 1946 ([Landau, 1946](#))([Ryutov, 1999](#)). The mathematical demonstration is rather subtle, and involves causality as a key element. The underlying physics idea can be understood by considering a particle with initial parallel velocity $v_{\parallel 0}$ in the presence of an electromagnetic field characterized by phase velocity, $v_{\phi} = \omega/k_{\parallel}$. A resonance occurs when the Cerenkov resonance condition, $\omega = k_{\parallel} v_{\parallel 0}$, is fulfilled. More precisely, during the process, particles with velocities near the wave phase velocity feel the wave effect, and see their motion modified in the synchronization process with the field. It can then be shown that in this case, the particle is either accelerated or decelerated with equal probability. As such, no net acceleration is imparted by the wave power. However, when considering an assembly of particles, the slower particles, i.e. those with $v_{\parallel 0} < \omega/k_{\parallel}$, which are accelerated, tend to feel the wave resonance with more intensity. On the other hand, those decelerated tend to resonate even less with the wave. Statistically, therefore, wave power will be employed to accelerate slower particles. The symmetrical situation involves faster particles, i.e. those with $v_{\parallel 0} > \omega/k_{\parallel}$. In contrast with the previous case, the decelerated particles will become more resonant than the accelerated ones. As a result, kinetic energy from the particles will tend to amplify the wave. However, fusion plasmas are typically characterized by Maxwellian distributions, which have

a decreasing dependence with parallel velocity, v_{\parallel} . The consequence is that slower particles are more numerous than faster particles, so that the net result of the two processes described previously is an absorption of the wave by the particles. This explains that γ , the wave damping rate, which characterizes the field attenuation with time, i.e. $E \propto \exp(-\gamma t)$, depends linearly on the slope of the distribution function considered at the wave-particle resonance, i.e. $\gamma \propto df_s/dv|_{v\phi}$. The result of this interaction on the distribution function of the interacting species is described by Eq. 4, and takes the form of a local flattening in velocity space around the resonance.

b) Cyclotron damping

Cyclotron damping is related to the process of Landau damping. The resonance condition, however, involves the particle gyromotion, and can be written as $\omega = p\Omega_{cs} + k_{\parallel}v_{\parallel}$, with p a non-zero integer. The cyclotron resonance occurs when the wave frequency matches the cyclotron frequency Ω_{cs} ($p=1$), i.e. the frequency characterizing the particle gyro-motion or one of its harmonics ($p>1$). The last term, $k_{\parallel}v_{\parallel}$, is the Doppler shift correction caused by the parallel motion of the particles along the field lines. Although it bears some similarities with Landau damping, the dependence of the cyclotron frequency with the confinement magnetic field magnitude, B_0 , induces essential differences in the resonance phenomenon. By construction, B_0 has a spatial dependence, proportional to $1/R$ (the distance to the torus revolution axis) in tokamaks – but more complex in stellarators. The result is that the resonance only occurs in a spatially localized region. The particles having periodical motion, the resonance occurs at multiple times as the particle travels through the plasma, which introduces another possible decorrelation mechanism in the system. The other fundamental difference is that the cyclotron motion is, by nature, perpendicular to the magnetic field. The resulting velocity-space diffusion occurs mainly in the perpendicular direction, which tends to increase the perpendicular particle velocities. The heated distribution functions in velocity space can therefore exhibit pronounced anisotropies, with a perpendicular energy content often significantly exceeding the parallel energy content.

3. Wave-induced current Drive

The process of RF-induced current drive (CD) is inherently linked to electron Landau damping. A wave characterized by angular frequency, ω , and parallel wavevector, k_{\parallel} , can resonate with electrons having a parallel velocity fulfilling the Cerenkov resonance condition, $v_{\parallel} = \omega/k_{\parallel}$. The consequent absorption of an energy quantum, $\Delta E = \hbar\omega$, by an electron results in an increase of its parallel momentum, $\Delta p_{\parallel} = \hbar k_{\parallel} = k_{\parallel}\Delta E/\omega$. Therefore, an injected wave characterized by an asymmetric spectrum in terms of k_{\parallel} will impart momentum to the electrons, thereby inducing a net parallel current.

As illustrative as this physics picture may be, it must be stressed that the mechanism of momentum transfer from the wave to the plasma described previously is not the dominant one in RF current drive applications. Indeed, it turns out that even waves imparting only perpendicular momentum to the electrons can drive current in a relatively efficient fashion. This results from the fact that wave-induced current drive relies for the most part on the variation of the plasma collisionality with the energy of resonant particles. Therefore, creating a population of electrons characterized by an excess of perpendicular energy can be exploited for current drive purpose, as long as the distribution function is asymmetric for the parallel velocity. This process is known as the Fisch-Boozer mechanism ([Fisch, 1987](#)).

A figure of merit of any current drive method is the amount of current driven, Δj , for a given amount of power expended, p . If we consider an electron receiving parallel momentum, Δp_{\parallel} , from the wave,

the corresponding current increase is $\Delta j = -e\Delta p_{\parallel}/m_e$, with e the absolute value of the electron charge and m_e the electron mass. Collisions, on the other hand, tend to oppose this momentum increase, a process which can be characterized by the counteracting force, $F = -v_e\Delta p_{\parallel}$, with v_e an effective collision frequency. By identifying the wave power spent to the work variation required to maintain the current drive process, we obtain the elemental current drive efficiency:

$$\Delta j/p = e/m_e v_e v_{\parallel}. \quad (7)$$

In order to maximize the efficiency, it would therefore seem natural to target thermal electrons, characterized by relatively low values of v_{\parallel} . Early current drive schemes, using *Alfvén waves*, were based on this idea. However, a large fraction of thermal electrons is trapped in the magnetic mirrors constitutive of the magnetic confinement structure, and therefore do not complete full revolutions in the toroidal direction. Consequently, they are unable to carry any parallel current and the resulting efficiency is too low to be of any interest. By contrast, in the range of velocities characterizing superthermal (or energetic) electrons, the effective collision frequency, v_e , varies as $(1/v_{\parallel})^3$, so that by virtue of Eq. 7, the efficiency increases with v_{\parallel}^2 . Finally, superthermal electrons also suffer less from trapping effects than thermal electrons. As a result, modern RF-based current drive schemes, i.e. those exploiting lower hybrid and electron cyclotron waves, are based on energetic electrons.

Finally, it should be noted that whereas Eq. 7 is interesting from a physics standpoint, it is hardly adequate to characterize the global efficiency of a given CD system, i.e. to obtain an estimate of the level of driven current corresponding to the power available on a given fusion device. For this purpose, it is worthwhile realizing that the absorbed power (in W) scales as $P_{abs} \sim 2\pi R \pi a_0^2 p_{abs}$, whereas the total current (in A) scales as $I_{CD} \sim \pi a_0^2 j$, with R the major radius, a_0 the minor radius, p_{abs} the power density (in $W.m^{-3}$) and j the current density (in $A.m^{-2}$). Accordingly, a useful quantity is the normalized current drive efficiency, a global figure of merit valid for any CD scheme and defined as $\eta_{CD} \equiv n_e R I_{CD} / P_{abs}$, with n_e the appropriately averaged electron density.

IV. Plasma heating & current drive by energetic ions

Regardless of the heating method employed, collisions often play an essential role since they are responsible for the transfer of power between the energetic particles and the thermal plasma species. Indeed, one of the most prevalent processes in modern heating and current drive applications involves the collisional relaxation of energetic ions, injected by the NBI system, born from fusion reactions or generated by RF acceleration of initially thermal species. The transfer of energy occurring between these energetic ions and the background plasma results from the various collisional processes at play. Their respective influence depends on the initial energies of the injected particles, E_f , on the Spitzer slowing-down time, τ_{se} , and on the critical velocity, E_c . It must be pointed out that energetic ions (NBI-driven, RF-driven or fusion products) can trigger instabilities, potentially inducing a radial redistribution of these ions. The impact of these processes on heating, current drive efficiency and fusion performance, as well as control schemes aimed at minimizing them (including using RF waves), is currently an active topic of experimental and numerical studies to prepare for the operation of next-step devices ([Gorelenkov and Sharapov, 2020](#)).

1. Neutral beam heating and current drive

Neutral beam injection is an auxiliary heating method which involves the production of high-energy ions in an accelerator, and their neutralization as they are ejected towards the confined plasma. These

neutral particles are immune to the effects of the magnetic field in which the plasma is confined, and can thus penetrate to the plasma core. They are progressively re-ionized as they travel through the hot plasma. Since they are injected at an energy much larger (typically in the range 50-150keV in ongoing devices, and 1MeV in ITER) than the typical confined plasma particle energies, they slow down through collisions with these particles. Adapted numerical codes ([Schneider et al., 2011](#)) taking into account the beam and plasma parameters are required to compute the neutral beam and corresponding power deposition. The NBI system installed in JET, as well as an illustration of a typical power deposition profile in the plasma is shown in *Figure 2*.

Consistently with the collisional relaxation process discussed in section “Kinetic theory elements”, the result of plasma heating by NBI ions depends on the background plasma and injected ion parameters. As an illustration, NBI ions with typical injection energies of $E_f \sim 100\text{keV}$ are used in JET and result in dominant thermal ion heating (see Table 1). In ITER, on the other hand, the plasma size and density make it necessary to resort to much higher beam energies to deposit the beam power in the plasma core. Negative NBI ions with $E_f \sim 1\text{MeV}$ have been adopted to fulfil this requirement, and tend to create a balanced heating on thermal electrons and ions, with little dependence on whether the background plasma consists of D ions only, or of mixed D-T fuel.

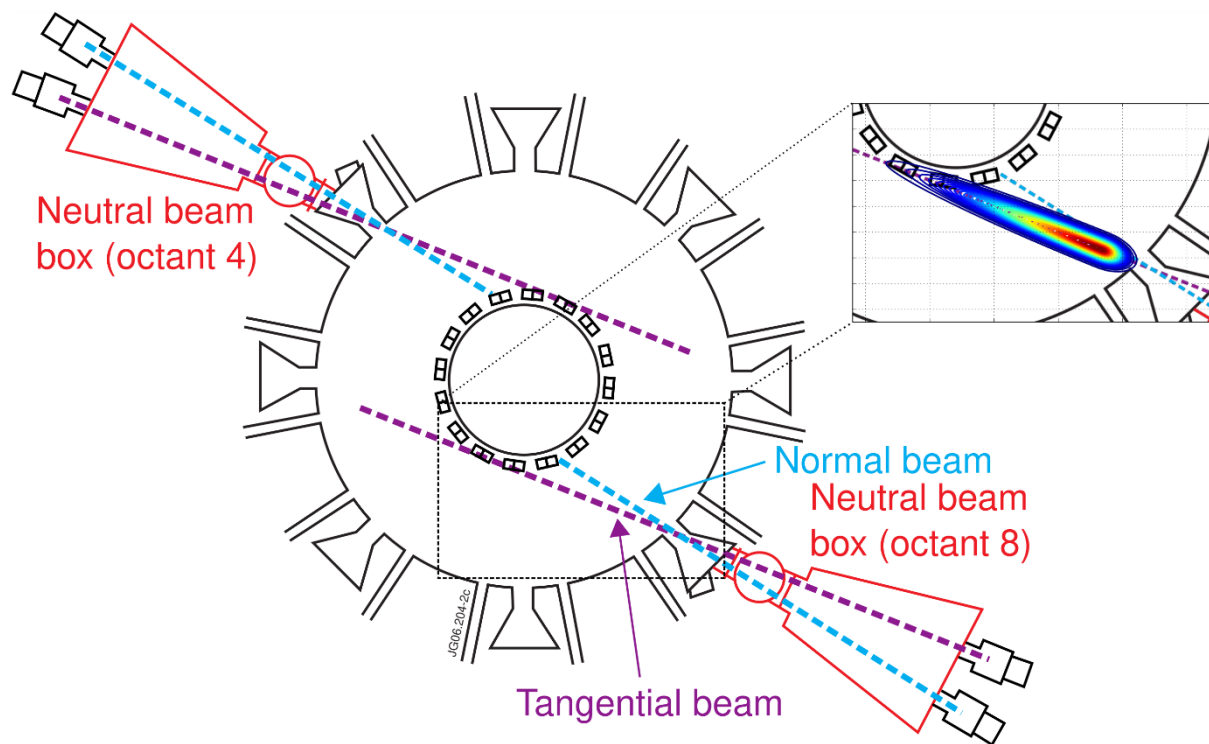


Figure 2: NBI heating in the JET tokamak. This device is equipped with two separate NBI injectors located in octants 4 and 8, each consisting of eight beams arranged in a tangential bank and a normal bank (Source: EUROfusion). In the inset is shown an illustration of the power deposition profile in the plasma corresponding to the tangential bank of the injector located in octant 8.

Background plasma / test particle	Initial energy [keV]	Critical energy [keV]	Spitzer time [s]	Thermalization time [s]	Fraction of power to ions / to electrons
JET D / D NBI	100	187	1.45	0.16	0.87 / 0.13
JET DT / DT NBI	100	206	1.81	0.18	0.89 / 0.11
ITER D / D NBI	1000	466	2.64	1.25	0.53 / 0.47
ITER DT / D NBI	1000	413	2.64	1.34	0.50 / 0.50

Table 1 : Main parameters relevant to the collisional relaxation of NBI ions in JET D, JET DT, ITER D, and ITER DT plasmas.

Depending on the NBI system geometry, in some situations, it is possible to inject energetic ions with a significant component of the velocity direction parallel to the confinement magnetic field, i.e. able to impart a significant amount of parallel momentum to the plasma. As a result, a finite level of toroidal current is driven, a scheme referred to as Neutral Beam Current Drive (NBCD). Assuming beam ions with mass, m_f , and density, n_f , the parallel momentum injected in the system is $m_f n_f \langle v_{\parallel} \rangle$, the average being performed on the (injected) energetic NBI ion distribution. Because of collisional relaxation, the beam ions will transfer this momentum to the background species through friction. Assuming, for simplicity a situation where $E_f \gg E_c$, this relaxation essentially takes place on electrons. The subsequent force on electrons in the parallel direction tends to increase their parallel momentum. In a stationary regime, the friction with thermal ions compensates this variation of parallel electron momentum. Taking into account the respective relaxation times of these processes and plasma quasi-neutrality, it can be shown that the resulting driven current takes the form $J_{NBCD} = J_f (1 - Z_f/Z_i)$, with $J_f = Z_f n_f e \langle v_{\parallel} \rangle$ the current carried by the beam ions, and Z_f (resp. Z_i) the charge number of beam (resp. thermal) ions. In many situations, Z_f and Z_i are comparable, which induces a large reduction in the NBI driven current because of the friction exerted by the background species on the energetic ions. A more accurate description of the process shows that the current drive efficiency predicted is generally larger than this analytical estimate. A first correction consists of taking into account trapped electron effects, which, in the case of NBCD, reduce the amount of electron current resulting from the cancellation of the beam current, and therefore entail an increase of the net efficiency (Fisch, 1987). The largest efficiency obtained to date is $\eta_{CD} = 0.155 \times 10^{20} \text{ A} \cdot \text{W}^{-1} \cdot \text{m}^{-2}$ using 360keV negative ion NBI in the JT-60U tokamak (Inoue et al., 2020). Predictions indicate that efficiencies of the order $\eta_{CD} \sim 0.2 - 0.4 \times 10^{20} \text{ A} \cdot \text{W}^{-1} \cdot \text{m}^{-2}$ should be achievable in ITER (Gomezano et al., 2007).

Finally, it must be pointed out that NBI also plays an essential role in driving toroidal rotation of the plasma, which is known to have a favorable effect on confinement (Jenko, 2020) and MHD stability (Lao et al., 2020) in ongoing devices. Predictions indicate that this effect will be less significant in reactor-scale devices, however. A larger plasma volume and density translates into a larger moment of inertia, whereas the higher beam ion energy results in a reduction of the injected torque.

2. Burning plasmas

Burning plasmas consist of a mix of D-T fuel, which produces alphas born at 3.5MeV able to heat the background species in a self-sufficient fashion (or nearly so). So far, only the tokamaks TFTR (USA) and JET (European Union) have operated with mixed D-T fuels. In these devices, the alpha power production remained small compared to auxiliary heating, making the effect of self-heating by alphas difficult to isolate. ITER is the first magnetic fusion device expected to contain a genuine burning plasma. In Table 2 are compared the situations in JET and in ITER with respect to plasma heating by the alphas. In the two cases, alphas predominantly heat the background electrons. However, the larger

density (and thus collisionality) in ITER high-performance scenarios results in a more balanced heating partition between the electrons and the fuel ions, which is favorable for plasma fusion performance.

Background plasma / test particle	Initial energy [keV]	Critical energy [keV]	Spitzer time [s]	Thermalization time [s]	Fraction of power to ions / to electrons
JET DT / alpha	3500	330	0.73	0.86	0.17 / 0.83
ITER DT / alpha	3500	826	1.32	1.00	0.35 / 0.65

Table 2 : Collisional plasma heating resulting from D-T alphas in JET and in ITER.

V. Plasma heating & current drive by radiofrequency waves

1. Ion Cyclotron (IC) Range of Frequency

In the Ion Cyclotron Range of Frequencies (ICRF, 20-80MHz), the antenna consists of a set of metallic straps enclosed in a box located at the edge of the magnetized medium and is capable of exciting a wave propagating in the plasma. In this frequency range, the system plasma-antenna must be considered as a global electrical circuit. This has the practical consequence that the antenna needs to be adapted to the plasma, by ensuring that their respective impedances match. In general, coupling ICRF power to the plasma is a delicate problem and a considerable effort is being devoted to this topic.

Examination of the dispersion relation in this range of frequencies reveals the existence of two waves, the so-called slow wave and fast magnetosonic wave. The slow wave, characterized by $N_{\perp}^2 \sim -\omega_{pe}^2 / \omega_{ci}^2$ is evanescent with a small wavelength ($\lambda < 1\text{mm}$), which means that it is useless for plasma heating since it cannot propagate away from the antenna vicinity. Here, $\omega_{ps}^2 = n_s q_s^2 / m_s \epsilon_0$ is the squared plasma frequency and $\omega_{ci} = Z_i e B_0 / m_i$ is the cyclotron frequency of the main ions. It should be noted that the slow wave plays an important role in the problem of wave coupling, and in the development of performance limiting electrical sheaths, which can occur in some situations. The fast wave dispersion relation for a cold plasma is given by $N_{\perp}^2 \sim (N_{//}^2 - R)(N_{//}^2 - L) / (S - N_{//}^2)$ with $R \sim -(c/v_a)^2 \omega_{ci} / (\omega - \omega_{ci})$, $L \sim (c/v_a)^2 \omega_{ci} / (\omega + \omega_{ci})$ and $S \sim -\omega_{pi}^2 / (\omega^2 - \omega_{ci}^2)$, v_a being the *Alfvén velocity*. It is clear from these expressions that the fast wave exhibits two cut-offs: the right cut-off, $N_{//}^2 = R$, the left cut-off, $N_{//}^2 = L$; and a resonance called the Alfvén (or hybrid) resonance, $N_{//}^2 = S$. The presence of the right cut-off implies that the fast wave does not propagate below a finite density, $n_e \sim 1 \times 10^{18} \text{m}^{-3}$, which corresponds to a location significantly inside the plasma scrape-off layer. In other words, like the slow wave, the fast wave is evanescent near the plasma edge. However, with a space decay typically of the order of 10cm, a significant fraction of the power can tunnel through the evanescence layer to reach the right cut-off, and propagate onward to the plasma core. The left cut-off, on the other hand, is located well inside the plasma core. Once coupled to the plasma, the fast wave is able to propagate between these two cut-offs, where it remains trapped until dissipation mechanisms damp the power.

The dominant damping mechanism of the fast magnetosonic wave is cyclotron damping by ions fulfilling the resonance condition, $\omega = p\omega_{ci} + k_{//}v_{//}$. The corresponding generic form of the quasilinear diffusion coefficient (see Eq. 6) is

$$D_{ql} = A \sum_p |E_{+J_{p-1}(k_{\perp}\rho_i)} + E_{-J_{p+1}(k_{\perp}\rho_i)}|^2 \delta(\omega - p\omega_{ci} - k_{//}v_{//}), \quad (8)$$

with E_{+} (resp. E_{-}) the left-handed (resp. right-handed) component of the electric field. J_p is the Bessel function of order p and $\rho_i = v_{\perp} / \omega_{ci}$ the (heated) ion Larmor radius. This expression shows that to lowest order, damping is determined by the left-handed component of the electric field, rotating in the ion

direction. Furthermore, for small arguments, $J_p(x) \sim x^p$. In other words, fundamental heating ($p=1$) is in principle very efficient since D_{q1} is at lowest order independent of $k_{\perp}\rho_i$. From a wave propagation standpoint, the situation described previously would seem to be ideal, since the cyclotron layer $\omega=\omega_{ci}$, around which the fundamental damping occurs, is always located between the two cut-offs. However, it turns out that the dispersion relation also dictates that the ratio of the left to right polarized components of the wave field be such as $E_+/E_=(N_{//}^2-R)/(N_{//}^2-L)$, which goes to zero as $\omega \rightarrow \omega_{ci}$. The result is that fundamental damping of the fast wave is a weak phenomenon, forbidding its applicability in a “pure” plasma, i.e. a plasma including a single ion species.

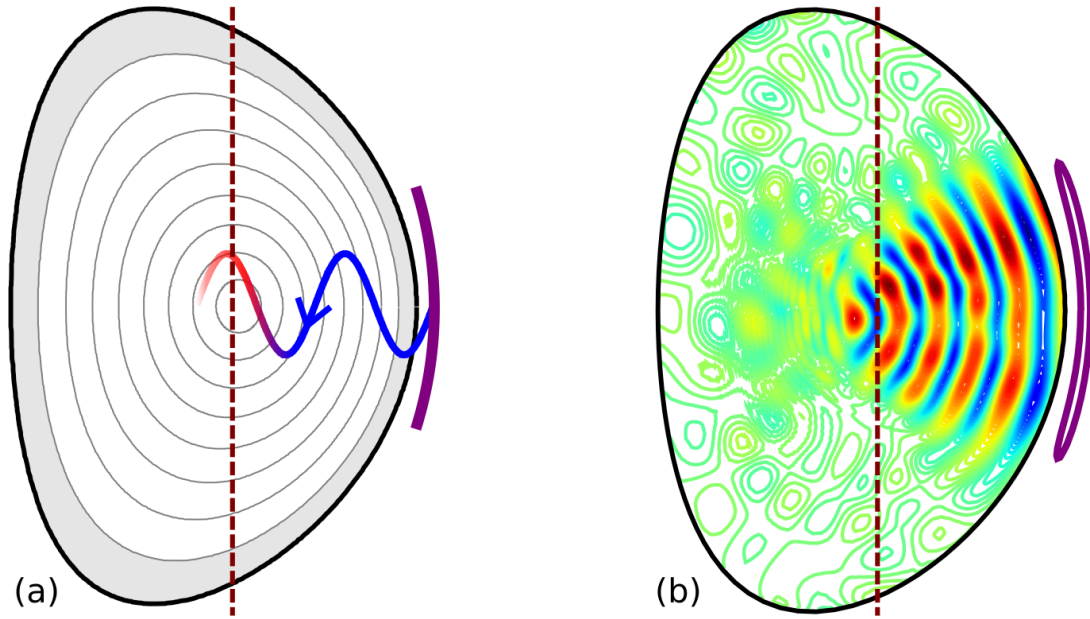


Figure 3: Depiction of IC wave heating in a tokamak plasma consisting of 95% deuterium+5% hydrogen. (a) General principle illustrated via a schematic wave propagating from the antenna across the plasma magnetic field surfaces (gray lines). The red color corresponds to locations where significant wave damping occurs; (b) Full-wave calculation of the left-handed electric field (shown in colour contours). The vertical dashed lines show the approximate location of the fundamental ion cyclotron resonance layer. Efficient wave absorption by the minority ions results in a low amplitude residual electric on the left of the resonance.

This problem can be overcome by using a harmonic of the cyclotron resonance, i.e. $p=2$ or more. This scheme, named harmonic heating, does not suffer from the same limitation as fundamental damping and can be used even in pure plasmas. However, Eq. 8 shows that the corresponding term is now proportional to $k_{\perp}\rho_i$, which depends itself on the pressure of the heated ion. To be efficient, second harmonic heating thus requires an already significant temperature of the heated ions. Nevertheless, second harmonic IC resonance heating (ICRH) has been successfully employed in various tokamaks as a heating method, and second harmonic tritium heating is a scenario which is planned to be used in ITER ([Gomezano et al., 2007](#)).

A possibility to exploit fundamental heating despite the limitation exposed previously is to introduce a small fraction (typically 2-8%) of a different ion in the plasma in addition to the majority ion and to perform fundamental cyclotron heating of this minority ion, hence the denomination: minority heating regime. In this case, it is possible to show that the left cut-off, $N_{//}^2=L$, and the hybrid resonance, $N_{//}^2=S$, are located very close to each other. The advantage is that the field polarization is now mainly imposed by the majority ion, and therefore E_+ does not cancel at the fundamental minority resonance. The second advantage is that the fundamental cyclotron layer, $\omega=\omega_{ci}$, is very close to the cut-off/hybrid

resonance couple. This results in a locally large electric field magnitude and associated stored reactive power. The outcome is efficient heating of the minority species, and this scheme has been routinely used in magnetic fusion devices for decades. The most widespread scenario is hydrogen heating in deuterium plasmas, with a typical hydrogen concentration of 3-5%. Since the power per absorbing ion is quite large, minority heating schemes tend to create very energetic ion populations and one relies on collisional relaxation on thermal electrons and/or ions for plasma heating. In ITER, fundamental heating of helium-3 (^3He) ions is currently one of the envisaged scheme to heat DT plasmas with ICRF waves. It is even envisaged to initiate the heating phase by injecting a small quantity of ^3He ions in the plasma. Minority damping, which is to lowest order independent of the heated ion temperature, will dominate and increase the ion temperature. Once the tritium temperature is sufficient and as the ^3He concentration naturally decreases, second harmonic tritium damping (located at the same position, since $\omega = \omega_{c3\text{He}} = 2\omega_{cT}$) is expected to take over, thus allowing smaller quantities of the expensive ^3He gas to be used. *Figure 3* illustrates the principle of ICRF heating in a tokamak such as JET, as well as an actual calculation of the left-handed electric field in a typical hydrogen minority heating scenario performed with a full wave code adapted to the description of waves in the Alfvén and IC range of frequencies ([Dumont, 2009](#)).

More recently, the so-called 3-ion scheme has been proposed and tested in several tokamaks ([Kazakov et al., 2017](#)). This involves the targeted heating of a third ion species characterized by charge number, Z , and mass number, A , in a plasma with two ion species (Z_1, A_1, Z_2, A_2). It can be shown that when the condition $Z_1/A_1 < Z/A < Z_2/A_2$ is satisfied, very efficient damping by the third species can be obtained, as long as it is present in very small concentrations (typically 0.1-1%). This scheme has been proposed to generate energetic ions in stellarators in order to experimentally document their confinement, and to provide efficient ICRF heating during phases of ITER operation at reduced magnetic field. It is also envisaged to use this scheme for ITER D-T plasmas, exploiting the natural presence of the beryllium (Be) impurity in the plasma. In a D-T mixture, Be satisfies $Z_T/A_T = 1/3 < Z_{\text{Be}}/A_{\text{Be}} = 4/9 < Z_D/A_D = 1/2$. The advantage is that the heavy Be ions tend to heat the fuel ions by collisions, rather than the electrons, which is beneficial in terms of fusion power production. It must be pointed out that, owing to its relatively novel character, this scheme is not as well established as the more traditional minority or harmonic heating schemes. Nevertheless, its flexibility and the fact that it proposes to exploit impurities naturally present in the plasma make it an appealing tool for future magnetic fusion devices.

A comparison of thermal plasma heating by typical RF-accelerated ions is shown in Table 3.

Background plasma / test particle	Initial energy [keV]	Critical energy [keV]	Spitzer time [s]	Thermalization time [s]	Fraction of power to ions / to electrons
JET D / H	2000	93	0.73	1.11	0.09 / 0.91
JET D / He3	700	280	0.54	0.29	0.49 / 0.51
ITER DT / He3	700	619	0.99	0.26	0.72 / 0.28
ITER DT / Be	700	1858	0.74	0.05	0.92 / 0.08

Table 3 : Collisional plasma heating resulting from RF-accelerated ions in JET and in ITER.

By increasing the minority concentration to $\sim 10\text{-}15\%$, the fundamental cyclotron layer, $\omega = \omega_{ci}$, on the one hand and the cut-off/resonance structure on the other hand move further apart. In this case, it is possible to have a substantial part of the fast wave power tunnel through the evanescence layer and undergo a mode conversion towards the pressure driven Ion Bernstein Wave (IBW). In this mode

conversion regime, one relies on the damping of the small wavelength IBW by the thermal electrons to obtain a localized electron heating source. It should be pointed out that despite good results obtained in several tokamaks, this scheme remains difficult to implement in practice, and requires delicate tuning of the magnetic field, minority concentration and antenna toroidal phase spectrum.

The reader should be aware that the physics of IC waves is very rich and many topics related to their use in fusion plasmas have been omitted. Among these, Fast Wave Electron Heating (FWEH) has been successful in some past experiments, and relies on the damping of the fast wave by the thermal electrons. FWEH is achieved by excluding all relevant cyclotron resonance layers by a careful choice of frequency/magnetic field combination. Using an asymmetric toroidal phase spectrum, furthermore, allows Fast Wave Current Drive (FWCD) to be achieved. FWEH is not envisaged in ITER, because the exclusion of all relevant cyclotron layers does not appear to be achievable in such a large device. FWCD, on the other hand, can be interesting since a moderate level of central non-inductive current can be obtained as a by-product of the IC heating wave damping on the electrons, simply by modifying the antenna current distribution and thus the toroidal phase spectrum. Other possibilities include MHCD (Minority Heating Current Drive), which relies on finite orbit width effects to drive a current related to the energetic ions; MCCD (Mode Conversion Current Drive) obtained by exciting a mode-converted wave with an asymmetric spectrum; HHFW (High Harmonic Fast Wave heating) relying on high frequency fast waves for localized electron heating/current drive, using traveling wave antennas to optimize wave coupling and toroidal directivity. To this day, these schemes are not considered as workhorse ICRH scenarios for ITER.

2. Lower Hybrid (LH) Range of Frequency

Between 1-10GHz, Lower Hybrid (LH) waves can be used for non-inductive current drive in tokamaks. In this frequency range, $\omega_{ci} \ll \omega \sim \omega_{LH} < \omega_{ce}$, with ω_{LH} the LH resonance frequency $\omega_{LH} \sim \omega_{pi} / (1 + \omega_{pe}^2 / \omega_{ce}^2)^{1/2}$. The cold dispersion relation reveals two waves: the fast wave already discussed for IC waves, is useless for plasma heating because the evanescence region between the antenna and the R-cut-off is too wide compared to the wavelength in this range of frequencies; the slow wave, on the other hand, is characterized by the approximate dispersion relation $N_{\perp}^2 \sim N_{//}^2 (m_p / m_e) \omega_{LH}^2 / (\omega - \omega_{LH})^2$. This expression shows that for given a magnetic field and density, the LH wave propagates at a finite angle, $\theta = \theta(\omega)$, with respect to the magnetic field direction. This kind of configuration is known as a resonance cone wave ([Swanson, 2003](#)). A further examination of the dispersion relation shows that the electric field polarization is essentially along the wave vector. The LH wave is therefore an electrostatic wave, and does not have any magnetic field component associated to it.

Originally, the idea was to target ion heating by damping of the wave near the LH resonance, hence the name of this scheme. Indeed, as discussed in section "Wave propagation", this cold resonance is characterized by $k_{\perp} \rightarrow \infty$, so that efficient heating of ions at relatively low velocities, $v_{\perp} \sim \omega / k_{\perp}$, (i.e. thermal) by perpendicular Landau damping was anticipated. However, experimental evidence pointed to several phenomena preventing this damping mechanism from taking place. For instance, the large values of N_{\perp} attained when approaching this resonance result in the parametric decay of the wave, a non-linear effect responsible for a degraded wave penetration in the plasma. Fortunately, it turns out that efficient wave damping by electrons satisfying the Cerenkov resonance, $v_{//} \sim \omega / k_{//}$, is also achievable in this range of frequencies, provided a slow wave with $N_{//}^2 > 1$ can be excited from an external antenna. Like the fast wave, the slow wave is subject to a low-density cut-off at $\omega \sim \omega_{pe}$, but the corresponding value is of the order 10^{17}m^{-3} in typical conditions. As a result, the evanescence

region is quite thin compared to the wavelength in vacuum, and it is possible to design efficient slow wave antennas with the required toroidal periodicity.

Once the slow wave has entered the plasma, it propagates towards the plasma center, with a corresponding increase of N_{\perp} . In this range of frequencies, however, if N_{\parallel} is smaller than a given N_{\parallel}^* which depends on density and magnetic field, a confluence between the fast and slow waves takes place in the plasma. Unless damping takes place before the slow wave reaches this confluence point, the converted fast wave propagates back towards the antenna. For all practical purposes, therefore, $N_{\parallel} > N_{\parallel}^*$ places a restriction on useful parallel refractive indices, densities and magnetic fields required for the slow wave to reach the plasma core (Brambilla, 1998), and is known as the Stix-Golant accessibility condition.

Typical values of the parallel refractive indices achieved with standard LH antennas are $N_{\parallel,ant} \sim 2$. For a plasma characterized by a core electron temperature, $T_e = 10 \text{keV}$, the range of velocities of the resonant electrons is therefore found to be $v_{\parallel}/v_{th,e} = c/(N_{\parallel}v_{th,e}) \sim 2.5$. For a Maxwellian distribution function, the corresponding number of electrons is very small. LH wave damping therefore relies on the changes of N_{\parallel} as it propagates. Indeed, it can be shown that various effects, among which are toroidicity and spectral broadening by density fluctuations, cause N_{\parallel} to vary during the propagation (Peysson et al., 2017). At some point, N_{\parallel} becomes sufficiently large for Landau damping by electrons with parallel velocities, $v_{\parallel} \sim v_{th,e}$, to take place. The regime in which the rays representative of the LH wave have to travel a long distance around the torus before damping is known as the multi-pass regime, and characterizes most past and current experiments using LH waves. If, on the other hand, T_e and/or N_{\parallel} are sufficiently large from the onset, the wave can be absorbed on its first pass onward the plasma core, a situation referred to as the single-pass regime, which is what would happen in a next-step tokamak containing a very hot plasma. Figure 4 illustrates the difference between these regimes in two discharges conducted in the Tore Supra tokamak, as computed with a Fokker-Planck code associated to a ray-tracing code (Decker, 2014).

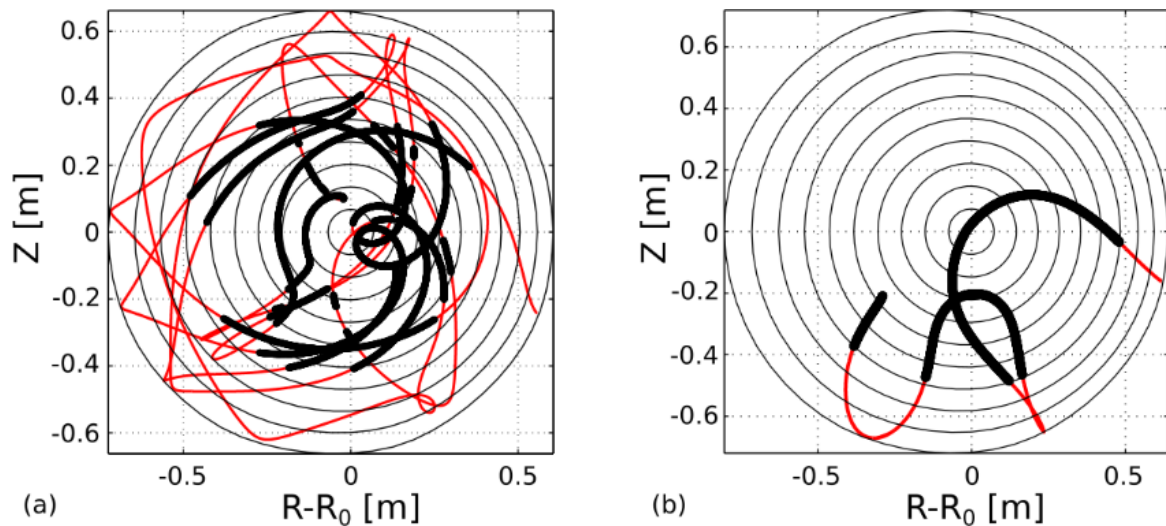


Figure 4: LH wave current drive in the Tore Supra tokamak. Ray trajectories are shown projected in the poloidal cross-section of the tokamak, but also propagate toroidally around the plasma. (a) In a relatively dense and cold plasma (volume averaged density $\langle n_e \rangle \sim 3.8 \times 10^{19} \text{m}^{-3}$, central temperature $T_{e0} \sim 2.4 \text{keV}$), the LH wave is in the multi-pass regime and the rays propagate on large distances before damping takes place. (b) In a less dense and hotter plasma, on the other hand ($\langle n_e \rangle \sim 1.3 \times 10^{19} \text{m}^{-3}$, $T_{e0} \sim 5.7 \text{keV}$), damping occurs relatively early during the propagation and the single-pass regime is approached.

In all cases, absorption initially occurs at large values of N_{\parallel} , and involves electrons close to the thermal velocity. An energetic electron tail is progressively created starting from these thermal electrons, eventually extending up to superthermal electrons at energies up to a few hundred keV. The quasilinear diffusion induced by the wave is in the parallel velocity direction. As a result, the electron distribution function features a flat region in terms of v_{\parallel} , known as the quasilinear plateau. Using an asymmetric N_{\parallel} spectrum therefore results in an asymmetric electron distribution function with respect to v_{\parallel} , with a substantial superthermal population. Electrons diffusing in the parallel direction do not experience trapping effects as much as electrons diffusing in the perpendicular direction. Furthermore, in addition to creating an asymmetric resistivity, the LH directly transfers parallel momentum to the electrons. These advantages explain the large LH current drive (LHCD) efficiency achieved in several devices, up to $\eta_{\text{LHCD}}=0.34 \times 10^{20} \text{A} \cdot \text{W}^{-1} \cdot \text{m}^{-2}$ in the large tokamaks JET and JT-60U. Projections for ITER predict that $\eta_{\text{LHCD}} \sim 0.24 \times 10^{20} \text{A} \cdot \text{W}^{-1} \cdot \text{m}^{-2}$ could be achieved, with a deposition profile peaked significantly off-axis (normalized radius ~ 0.7) because of the high density and temperature ([Gomezano et al., 2007](#)). Despite these results, at this point, uncertainties related to the LH wave penetration and current drive efficiency in dense plasmas, as well as parasitic wave damping by the fusion alphas in a D-T plasma, make their future applicability in reactors uncertain.

3. Electron Cyclotron (EC) Range of Frequency

Electron Cyclotron (EC) waves are typically injected in the frequency range 50-200GHz, which coincides with the fundamental cyclotron resonance of electrons in most modern magnetic fusion devices. Lower field operation opens the possibility to use harmonic schemes. In this frequency range, $\omega_{\text{ci}} \ll \omega \sim \omega_{\text{ce}} \sim \omega_{\text{pe}}$. The wave is exclusively damped by resonant electrons. For these frequencies/wavelengths, the propagation is quasi-optical and is quite adequately described by ray-tracing or beam-tracing codes. This has the considerable practical advantage of allowing a coupling of the wave to the plasma using an antenna located at some distance, generally consisting of a set of steerable mirrors to vary the deposition location, and possibly to use these waves for current drive by injecting them obliquely with respect to the magnetic field.

The dispersion relation reveals two distinct waves, called the ordinary and extraordinary modes. The ordinary (O) mode has the simple dispersion relation, $N_{\perp}^2 = 1 - \omega_{\text{pe}}^2 / \omega^2$, showing that it can propagate to the plasma core, at least up to the plasma cut-off, $\omega = \omega_{\text{pe}}$, which corresponds in practice to central densities larger than 10^{20}m^{-3} . Fundamental absorption of the ordinary mode is therefore a viable scheme for most tokamaks, including ITER. The extraordinary (X) mode has the somewhat more complex dispersion relation, $N_{\perp}^2 = (\omega^2 - \omega_{\text{R}}^2)(\omega^2 - \omega_{\text{L}}^2) / (\omega^2(\omega^2 - \omega_{\text{UH}}^2))$, with ω_{R} and ω_{L} the right and left cut-off frequencies, and ω_{UH} the upper hybrid frequency. The right cut-off prevents the X-mode from reaching the fundamental cyclotron resonance, $\omega = \omega_{\text{ce}}$, from the low field side of the plasma. Although conceptually appealing, the solution of installing an antenna on the high field side does not appear to be realistic in the context of a reactor. Alternatively, one can resort to the second harmonic resonance $\omega = 2\omega_{\text{ce}}$. The drawback of this method is that the right cut-off, while not preventing the resonance at $\omega = 2\omega_{\text{ce}}$ from being reached, imposes a cut-off density which is only 50% of the cut-off density of the O-mode for a given frequency and therefore requires operating a relatively higher frequency. The two schemes envisaged for EC resonance heating (ECRH) and current drive (ECCD) in modern magnetic fusion devices are therefore fundamental ordinary mode heating (O-1) or second harmonic extraordinary mode heating (X-2), and sometimes even third harmonic X-mode heating (X-3).

The fundamental resonance condition for EC waves is given by $\omega = \omega_{ce} + k_{\parallel} v_{\parallel}$, where $\omega_{ce} = eB_0 / \gamma m_e$ is the electron cyclotron frequency and γm_e is the electron mass corrected for relativistic effects, which turn out to play a major role in the resonance condition. It can be shown that the resonance curve is an ellipse in velocity or momentum space, $(p_{\perp}, p_{\parallel})$, with $\mathbf{p} = \gamma m_e \mathbf{v}$ the electron momentum. Writing $\omega = \omega_{ce}(R_{res})$, with R_{res} the resonant position in terms of major radius R , shows that the energy of resonant electrons is given by:

$$E = m_e c^2 (R_{res}/R - 1 + N_{\parallel} p_{\parallel} / m_e c). \quad (9)$$

For a given position, R , the resonance parameters ω / ω_{ce} and N_{\parallel} thus locate the interaction in the $(p_{\perp}, p_{\parallel})$ plane, which results in a coupling between the wave damping properties in physical space and the location of distribution function modifications induced by the wave momentum space. The quasilinear diffusion that is induced occurs mainly in the perpendicular direction near the resonance ellipse.

Studying wave damping more carefully requires the calculation of the full hot relativistic dielectric tensor (Brambilla, 1998). Some insight into the damping process can nevertheless be gained by realizing that for EC waves, the electric field-dependent coefficient in the quasilinear diffusion coefficient (Eq. 6) is, to lowest order, proportional to $|d^{(p)}(\mathbf{E})| \sim |v_{\perp} E J_{p-1}(k_{\perp} \rho_e)|^2$, with E the right-handed component of the electric field, J_{p-1} the Bessel function of order $p-1$ and ρ_e the electron Larmor radius. For small arguments, $J_{p-1}(k_{\perp} \rho_e) \sim (k_{\perp} \rho_e)^{p-1}$, showing that fundamental damping does not depend directly on the electron temperature, whereas second harmonic damping is a finite temperature effect. This would seem to indicate that O-1 damping is more efficient than X-2 damping, but, as for IC waves, the electric field polarization near $\omega = \omega_{ce}$ is such that E is relatively small (0 in the cold-plasma approximation), thereby decreasing the absorption strength. This is confirmed by comparing the respective optical depths for the O-1 and X-2 modes, i.e. the ratio between the power crossing the resonance layer and the incident power, which shows that X-2 damping is typically 5-10 times more efficient than O-1 damping. It should be pointed out that despite this difference, this damping is very efficient in both cases, so that the power deposition profiles are essentially always narrow.

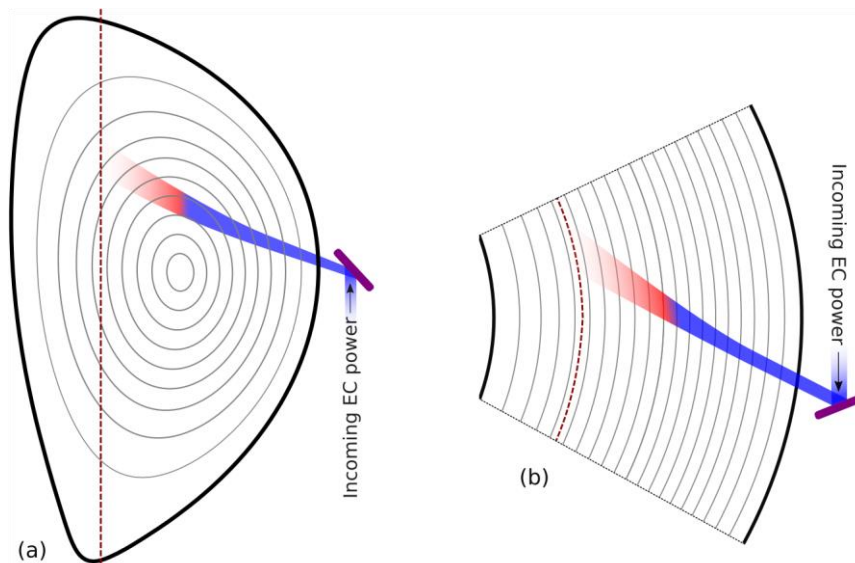


Figure 5: Schematic of EC wave heating and current drive in a tokamak such as ITER. (a) Poloidal cut; (b) Top view. The beam is shown in blue, with red colouring at locations where significant absorption occurs. The (fictitious) EC steering mirror is shown in magenta, and is used in this representation to inject the wave with a toroidal angle with respect to the magnetic field direction, a situation typical of ECCD. The red dashed curve shows the cold EC resonance.

Furthermore, as explained previously, EC antennas are composed of steerable mirrors (Farina, 2014). As a result, it is straightforward to inject the wave with a certain angle with respect to the magnetic field to 1) locate the damping at a precise position in radius, and 2) drive a finite toroidal current. This is illustrated in *Figure 5*. As discussed in section “Wave propagation”, even though no parallel momentum is imparted by an EC wave to the plasma since the quasilinear diffusion is in the perpendicular direction, the Fisch-Boozer mechanism still makes EC waves suitable for current drive applications. Successful ECCD in a tokamak requires that the damping take place before the fundamental resonance, so that, by virtue of Eq. 9, it occurs on significantly energetic electrons. In theory, the achievable CD efficiency is only a factor of $\frac{3}{4}$ lower than that attained with LH waves (the difference being due to the absence of any parallel momentum input). However, owing to trapped electron effects and to the relatively modest energies of resonant electrons, ECCD is significantly less efficient than LHCD, except at very high temperatures. The record ECCD efficiency to date, $\eta_{\text{ECCD}}=0.042 \times 10^{20} \text{A.W}^{-1}.\text{m}^{-2}$, was obtained in JT-60U. In ITER, the EC launcher geometry and plasma parameters should allow $\eta_{\text{ECCD}} \sim 0.2 \times 10^{20} \text{A.W}^{-1}.\text{m}^{-2}$ to be achieved ([Gomezano et al., 2007](#)). The good localization of the deposition and the excellent flexibility offered by the injector arguably compensate for this lower global efficiency – the driven current density being locally quite large at a position chosen by an operator or by an automated control system. For this reason, EC waves have a wide range of applications, including current profile control, MHD control, and plasma start-up assist (required for stellarators, useful in large tokamaks to enlarge the domain of parameters for plasma breakdown), and their exploitation should increase further as the technological development of efficient and powerful EC generators advances.

Acknowledgements

Careful manuscript reading and insightful comments by M. Schneider, G. Giruzzi, D. Keeling and Y. Peysson are gratefully acknowledged.

References

- Brambilla, M., 1998. *Kinetic Theory of Plasma Waves*. Oxford: Clarendon Press.
- Decker, J., Peysson, Y., Artaud, J.-F., Nilsson, E., Ekedahl, A., Goniche, M., Hillairet, J., and Mazon, D., 2014. Damping of lower hybrid waves in large spectral gap configurations. *Physics of Plasmas*, 21(9), p.092504.
- Dumont, R., 2009. Variational approach to radiofrequency waves in magnetic fusion devices. *Nuclear Fusion*, 49(7), p.075033.
- Farina, D., Henderson, M., Figini, L. and Saibene, G., 2014. Optimization of the ITER electron cyclotron equatorial launcher for improved heating and current drive functional capabilities. *Physics of Plasmas*, 21(6), p.061504.
- Fisch, N., 1987. Theory of current drive in plasmas. *Reviews of Modern Physics*, 59(1), pp.175-234.
- Goldston, R., and Rutherford, P., 1995. *Introduction to Plasma Physics*. Bristol: Institute of Physics Publishing.
- Gorelenkov, N. and Sharapov, S., 2020. Magnetic Confinement Fusion - Plasma Theory: Energetic Particle Physics. Chapter 01208, this encyclopedia.

- Gormezano, C., Sips, A., Luce, T., Ide, S., Becoulet, A., Litaudon, X., Isayama, A., Hobirk, J., Wade, M., Oikawa, T., Prater, R., Zvonkov, A., Lloyd, B., Suzuki, T., Barbato, E., Bonoli, P., Phillips, C., Vdovin, V., Joffrin, E., Casper, T., Ferron, J., Mazon, D., Moreau, D., Bundy, R., Kessel, C., Fukuyama, A., Hayashi, N., Imbeaux, F., Murakami, M., Polevoi, A. and John, H., 2007. Chapter 6: Steady state operation. *Nuclear Fusion*, 47(6), pp.S285-S336.
- Helander, P., and Sigmar, D., 2005. *Collisional Transport in Magnetized Plasmas*. Cambridge: Cambridge University Press.
- Inoue, T. et al., 2020. Magnetic Confinement Fusion - Technology: 'Plasma Engineering'. Chapter 01214, this encyclopedia
- Jenko, F., 2020. Magnetic Confinement Fusion - Plasma Theory: Transport and Confinement. Chapter 01205, this encyclopedia.
- Kazakov, Y., Ongena, J., Wright, J., Wukitch, S., Lerche, E., Mantsinen, M., Van Eester, D., Craciunescu, T., Kiptily, V., Lin, Y., Nocente, M., Nabais, F., Nave, M., Baranov, Y., Bielecki, J., Bilato, R., Bobkov, V., Crombé, K., Czarnecka, A., Faustin, J., Felton, R., Fitzgerald, M., Gallart, D., Giacomelli, L., Golfinopoulos, T., Hubbard, A., Jacquet, P., Johnson, T., Lennholm, M., Loarer, T., Porkolab, M., Sharapov, S., Valcarcel, D., Van Schoor, M. and Weisen, H., 2017. Efficient generation of energetic ions in multi-ion plasmas by radio-frequency heating. *Nature Physics*, 13(10), pp.973-978.
- Landau, L., 1946. On the vibrations of the electronic plasma. *J. Phys. USSR*, 10, p.25.
- Lao, L. et al., 2020. Magnetic Confinement Fusion - Plasma Theory: Magnetohydrodynamic Stability. Chapter 01206, this encyclopedia.
- Peysson, Y., Bonoli, P., Chen, J., Garofalo, A., Hillairet, J., Li, M., Qian, J., Shiraiwa, S., Decker, J., Ding, B., Ekedahl, A., Goniche, M. and Zhai, X., 2017. Current Challenges in the First Principle Quantitative Modelling of the Lower Hybrid Current Drive in Tokamaks. *EPJ Web of Conferences*, 157, p.02007.
- Ryutov, D., 1999. Landau damping: half a century with the great discovery. *Plasma Physics and Controlled Fusion*, 41(3A), pp.A1-A12.
- Sarazin, Y., 2020. Magnetic Confinement Fusion – Plasma Theory: Kinetic and Fluid Analysis. Chapter 01204, this encyclopedia.
- Schneider, M., Eriksson, L., Jenkins, I., Artaud, J., Basiuk, V., Imbeaux, F. and Oikawa, T., 2011. Simulation of the neutral beam deposition within integrated tokamak modelling frameworks. *Nuclear Fusion*, 51(6), p.063019.
- Stix, T., 1992. *Waves in plasmas*. New York: Springer-Verlag.
- Swanson, D., 2003. *Plasma Waves*. Second edition. Bristol: Institute of Physics Publishing.
- Wesson, J., 2011. *Tokamaks*. Fourth edition. Oxford: Oxford University Press.
- Yamada, H., 2020. Magnetic Confinement Fusion – Experimental physics: Stellarators. Chapter 01211, this encyclopedia.
- Zohm, H., 2020. Magnetic Confinement Fusion – Experimental physics: Tokamaks. Chapter 01210, this encyclopedia.

Glossary

- **Alfvén velocity:** The group and phase velocities associated to Alfvén waves are of the order of the Alfvén velocity, $v_a = B_0 / (\mu_0 n_i m_i)^{1/2}$, with B_0 the confining magnetic field, μ_0 the vacuum permeability and n_i (resp. m_i) the ion density (resp. mass). This ratio reflects the antagonistic effects of the magnetic field line tension on the one hand, and of the ion inertia on the other hand.
- **Alfvén waves:** A kind of magnetohydrodynamic wave characterized by a periodic oscillation of the plasma ion drift motion associated to a perturbation of the magnetic field. It is characterized by a frequency much lower than the ion cyclotron frequency. Alfvén waves play an important role in magnetic fusion plasmas because they can interact efficiently with energetic ions and, in some situations, induce a radial displacement of these particles ([Gorelenkov and Sharapov, 2020](#)).
- **Boltzmann equation:** A kinetic equation describing statistical properties of a thermodynamic system out-of-equilibrium. In practice, the generic form of the collision term appearing in this equation prevents it from being directly applied to fully ionized plasmas in which long-range Coulomb collisions dominate.
- **Bootstrap current:** A contribution to the toroidal plasma current resulting from the fact that the plasma pressure is maximal near the plasma center and decreases towards the edge. Because of this non-uniformity, the friction between trapped electrons and passing electrons results in a net transfer of parallel momentum from the former to the latter, inducing a finite parallel current ([Helander and Sigmar, 2005](#)). In tokamaks, the (beneficial) bootstrap contribution to the total current can be quite significant (typically ~50% in ITER, depending on the regime of operation).
- **Coulomb logarithm:** This quantity appears in the theory of Coulomb collisions taking place between the charged particles comprising a plasma. Denoting Λ the approximate number of particles contained in the Debye sphere, its logarithm, $\ln(\Lambda)$, is much larger than unity in weakly coupled plasmas, in which collective effects dominate ([Goldston and Rutherford, 1995](#)). Fusion plasmas are examples of weakly coupled plasmas and it is found that $\ln(\Lambda)$ ranges from ~17 (current fusion experiments) to ~18 (fusion reactors).
- **Fokker-Planck equation:** An equation deduced from the Boltzmann equation assuming that long-range collisions dominate, as is appropriate in hot magnetic fusion plasmas. The ensuing accumulation of multiple small angle deviations for a given particle results in a diffusion equation for the distribution function in velocity space.
- **keV:** In magnetic fusion plasmas, it is customary to express energies in terms of electronvolt (eV), kilo-electronvolt (keV) or mega-electronvolt (MeV). 1eV is approximately equivalent to 1.602176×10^{-19} Joule. By extension, this unit is also employed for plasma temperatures: 1eV is approximately equivalent to 1.160450×10^4 Kelvin.
- **Quasilinear equation:** A kinetic equation describing the secular (i.e. long duration) effect of the interactions taking place between an electromagnetic wave and the plasma particles. It is obtained by averaging the Vlasov equation over a time much longer than the wave period, and over a space region with a large extension compared to the wavelength.
- **Trapped /passing particles:** In a magnetic confinement device, the confining magnetic field B_0 is non-uniform. The velocity vector, \mathbf{v} , of a given particle of mass, m , can be written in terms of parallel (v_{\parallel}) and perpendicular (v_{\perp}) components with respect to the magnetic field direction.

Magnetic confinement imposes that the particle kinetic energy, $E=m(v_{\parallel}^2+ v_{\perp}^2)/2$, and its magnetic moment, $\mu=mv_{\perp}^2/(2B_0)$, be conserved to lowest order. By manipulation of these two equations, it can be demonstrated that particles can be classified into two main categories: some are characterized by trajectories with $v_{\parallel}\neq 0$ at any point, whereas others periodically see their parallel velocity cancel. The former are passing particles, and perform complete toroidal revolutions. The latter, on the other hand, travel back and forth in the toroidal direction and are called trapped particles. In particular, trapped electrons do not carry any toroidal current.

- **Vlasov equation:** A kinetic equation obtained by neglecting inter-particle correlations in the kinetic description of the plasma, i.e. assuming that all particle interactions are mediated by a self-consistent average electromagnetic field satisfying Maxwell's equations. Since collisions are neglected in this process, this equation is applicable to timescales much smaller than the typical collision time. It is sometimes referred to as the collisionless Boltzmann equation.

- **WKB (Wentzel-Kramers-Brillouin) approximation:** A special case of multiple scale analysis. In the context of waves propagating in plasmas, it is relevant when the plasma varies on a space scale much larger than the wavelength. In this case, at a given position x , the electromagnetic field can be written in the form of $E(x)=E_0(x)\exp(iS(x))$, where $E_0(x)$ is assumed to vary slowly compared to the phase $S(x)$. It is applicable outside of wave cut-offs or resonances ([Swanson, 2003](#)).